Original Article
Prostate cancer

The World Journal of
MEN's HEALTH

Check for updates

Comparative Analysis of Proteomes and Phosphoproteomes in Patients with Prostate Cancer Using Different Surgical Conditions

Hee-Sung Ahn[1] , Jeonghun Yeom[2] , Hwangkyo Jeong[3] , Won Young Park[4] , Ja Yoon Ku[5] , Byeong Jin Kang[6] , Kyung Hwan Kim[6] , Chan Ho Lee[7] , Sangheon Song[8] , Sun Sik Bae[9] , Kyunggon Kim[1,2,10,11] , Hong Koo Ha[6,12]

[1]Asan Institute for Life Sciences, Asan Medical Center, [2]Convergence Medicine Research Center, Asan Institute for Life Sciences, [3]Department of Biomedical Sciences, University of Ulsan College of Medicine, Asan Medical Center, [4]Department of Pathology, Seegene Medical Foundation, Seoul, [5]Department of Urology, Dongnam Institute of Radiological & Medical Sciences Cancer Center, [6]Department of Urology, College of Medicine, Pusan National University, [7]Department of Urology, Inje University Busan Paik Hospital, Inje University College of Medicine, [8]Department of Internal Medicine, School of Medicine, Pusan National University, [9]Department of Pharmacology, School of Medicine, Pusan National University, Busan, [10]Digestive Diseases Research Center, University of Ulsan College of Medicine, [11]Bio-Medical Institute of Technology, Asan Medical Center, Seoul, [12]Biomedical Research Institute, Pusan National University Hospital, Busan, Korea

Purpose: To establish the standard of procedure in preparing benign and cancerous prostate tissues and evaluate the quality of proteomics and phosphoproteomics during transurethral resection of the prostate (TUR-P) with different surgical conditions.
Materials and Methods: TUR-P tissue samples from three patients, two diagnosed with prostate cancer and one with benign prostatic hyperplasia, were each analyzed under three different conditions, based on differences in energy values, tissue locations, and surgical techniques. Global- and phosphorylated proteomic profiles of prostate tissues were analyzed by liquid chromatography-tandem mass spectrometry.
Results: A total of 6,019 global proteins and 4,280 phosphorylated peptides were identified in the nine tissues. The quantitative distributions of proteins and phosphorylation in tissues from the same patient were not affected by changes in the surgical conditions, but indirect relative comparisons differed among patients. Phosphorylation levels, especially of proteins involved in the androgen receptor pathway, important in prostate cancer, were preserved in each patient.
Conclusions: Proteomic profiles of prostate tissue collected by TUR-P were not significantly affected by energy levels, tissue location, or surgical technique. In addition, since protein denaturation of samples through TUR-P is rarely confirmed in this study, we think that it will be an important guide for tissue samples in castration resistant prostate cancer patients, where it is difficult to obtain tissue. This result is the first report about proteomic and phosphoproteomic results with TUR-P samples in prostate cancer and will be theoretical basis in protein analysis research with prostate cancer tissues.

Keywords: Mass spectrometry; Prostatic hyperplasia; Prostatic neoplasm; Proteme; Transurethral resection of prostate

INTRODUCTION

Prostate cancer (PCa) is the fifth leading cause of death worldwide in men and the second most frequent cancer diagnosis in men in 112 countries [1]. According to GLOBOCAN 2020 estimates, 1,414,259 men worldwide were newly diagnosed with PCa in 2020 [1]. PCa may be asymptomatic during its early stages and often has an indolent course, which may require only active surveillance.

Men are screened for PCa by measuring the serum concentration of prostate-specific antigen (PSA) [2]. Men with high PSA concentrations, usually >4 ng/mL, undergo prostate biopsy to confirm the diagnosis of PCa. High PSA, however, is not a specific marker of PCa, indicating a need for new biomarkers diagnostic of PCa. Analysis of protein samples may enable identification of the pathological signal and subtype of PCa and administration of drugs appropriate to each patient [3]. Many molecular-level mechanisms for multiomics, especially proteomics, analysis of specimens have been developed [4]. Although prostate tissue specimens can be collected by prostate biopsy, the limitation of biopsy samples is that they are very small. Instead of biopsy, tissue can be obtained with transurethral resection of the prostate (TUR-P). Samples obtained from TUR-P are usually much larger and we can get the tissues in patients with castration resistant prostate cancer (CRPC). Because of Electric current during TUR-P, this current may cause protein denaturation at the surface of the tissue. To our knowledge, however, no studies to date have describes about changes in proteins after TUR-P and sample preparation for this analysis with prostate tissues.

In the present study, we want to confirm the possibility of obtaining prostate tissue including CRPC through TUR-P and to establish a standard of protocol for proteomic and phosphoproteomic analysis. To reveal the possibility, prostate tissue samples were collected from three patients, two with PCa including CRPC and one with benign prostatic hyperplasia (BPH), under three different conditions to determine whether differences in surgical parameters, tissue locations, and TUR-P energies used to collect samples affected global and phosphorylated proteins. This study found that the differences among the three conditions within individuals were not greater than the differences among the three subjects.

MATERIALS AND METHODS

1. Ethics statement

The study protocol was approved by the Institutional Review Board of Pusan National University Hospital (PNUH-IRB No. 1802-004-063), which waived the requirement for informed consent. The prostate biospecimens and data used for this study were provided by the Biobank of Pusan National University Hospital (Busan, Korea), a member of the Korea Biobank Network.

2. Clinical samples

Tissue samples from one patient with BPH and two with PCa containing at least 80% adenocarcinoma of the prostate, characterized according to National Comprehensive Cancer Network (NCCN) risk [5], were examined by a uro-pathologist (WYP) to confirm the original diagnosis. These tissue samples, collected at the Biobank of Pusan National University Hospital by TUR-P (ForceTriad Energy Platform; Medtronic Limited, Minneapolis, MN, USA), had been snap frozen and stored at -80°C within 30 minutes after TUR-P. During TUR-P, the cutting current power was set at 0 W, 40 W, or 60 W, and the coagulation current power at 0 W or 40 W. The TUR-P was performed with a 24F continuous irrigation flow resectoscope (Karl Storz, Tuttlingen, Germany), a 30 degree angled optical lens (Karl Storz), a tungsten wire loop electrode (Karl Storz), and mannitol/sorbitol solution (Urosol, CJ Parma, Seoul, Korea). All the samples from PCa were collected in patients showing radiologic or PSA progression during androgen deprivation therapy.

3. Surgical parameters

Electro-resection in monopolar TUR-P was performed using a tungsten wire loop, with a cutting power of 40 W or 60 W and a coagulation power of 0 W or 40 W (blend mode). Tissue was extracted from CPRC patient #1 (Pt1) at the same location by altering the cutting and coagulation currents during TUR-P. Current was initially set at 40 W for cutting and 0 W for coagulation, then at 60 W for cutting and 0 W for coagulation, and finally at 60 W for cutting and 40 W for coagulation. Tissue was extracted from BPH patient #2 (Pt2) at three different locations, with a fixed current of 40 W for cutting and 60 W for coagulation. Tissue was extracted from PCa patient #3 (Pt3) at a fixed current of

60 W for cutting and 0 W for coagulation; the sample was divided into two portions, the outer side with heat damage, and the inner side without heat damage.

4. Protein extraction, enzymatic digestion, and phosphorylated peptide enrichment

Tissue samples were suspended in lysis buffer (8 M urea, 50 mM ammonium bicarbonate, 1× Halt™ protease inhibitor cocktail, 0.1% benzonase nuclease, pH 8.0), lysed for 1 minute with the probe sonicator (VCX-130; Sonics and Materials Inc., Newtown, CT, USA) at an amplitude of 28% in pulse mode (1 s on/2 s off), and centrifuged at 18,000 ×g for 10 minutes at 4°C. The protein concentration of each supernatant containing extracted proteins was measured with a BCA protein quantification kit (Pierce™ BCA Protein Assay Kit; cat. No.: 23225; Thermo Fisher Scientific, Waltham, MA, USA). A 500 μg aliquot of proteins was dissolved in 500 μL of lysis buffer, mixed 1:1 with 20 mM tris(2-carboxyethyl)phosphine hydrochloride (TCEP) (final concentration, 10 mM TCEP), and incubated for 1 hour at room temperature. IAA was added to a final concentration of 40 mM and the samples were alkylated by incubation for 1 hour in the dark at room temperature. The samples were diluted 1:10 with 50 mM ABC and incubated with a 1:25 mixture of trypsin/Lys-C (enzyme:sample) for 16 hours at 37°C. The digestion reaction was stopped by the addition of formic acid to a final concentration of 0.3%. The peptide mixtures were desalted with a Sep Pak C-18 cartridge (Waters, Milford, MA, USA), lyophilized with a cold trap (CentriVap Cold Traps; Labconco, Kansas City, MO, USA), and stored at -80°C until used. Of each peptide sample, 95% was used for TiO$_2$ enrichment for phosphoproteomic analysis and the remaining 5% was used for global proteomic analysis. TiO$_2$ enrichment was performed as described by the manufacturer (Titansphere Phos-TiO kit; Cat. No. 5010-21309; GL Sciences, Tokyo, Japan) and the samples were cleaned with graphite spin columns (Pierce® Graphite Spin Columns; cat. No.: 88302; Thermo Fisher Scientific).

5. Liquid chromatography-tandem mass spectrometry

Peptides were separated using the Dionex UltiMate 3000 RSLCnano system (Thermo Fisher Scientific). Each dried sample was reconstituted with 25 μL 0.1% formic acid, a 5 μL aliquot of which was injected into a C18 Pepmap trap column (20 mm×100 μm i.d., 5 μm, 100 Å; Thermo Fisher Scientific) and separated by an Acclaim™ Pepmap 100 C18 column (500 mm×75 μm i.d., 3 μm, 100 Å; Thermo Fisher Scientific) over 200 minutes (250 nL/min) using a 0% to 48% acetonitrile gradient in 0.1% formic acid and 5% DMSO for 150 minutes at 50°C. The liquid chromatography column was coupled to a Q Exactive mass spectrometer (Thermo Fisher Scientific) with a nano-ESI source. Mass spectra were acquired in a data-dependent mode with an automatic switch between a full scan and 20 data-dependent MS/MS scans. The target value for the full scan MS spectra was 3,000,000 with a maximum injection time of 100 ms and a resolution of 70,000 at m/z 400. The ion target for MS/MS was set to 1,000,000 with a maximum injection time of 50 ms and a resolution of 17,500 at m/z 400. Repeated peptides were dynamically excluded for 20 seconds.

6. Proteomic identification and quantification

The acquired MS/MS spectra were retrieved on the SequestHT on Proteome discoverer (version 2.2; Thermo Fisher Scientific) and compared with the SwissProt human protein sequence database (May 2017). Precursor mass tolerance was set to ±10 ppm and MS/MS tolerance was set at 0.02 Da. The search parameters were set to default parameters, including cysteine carbamidomethylation as a fixed modification, and N-terminal acetylation, methionine oxidation and phospho-serine, -threonine, and -tyrosine as variable modifications with two miscleavages. False discovery rates were set at 1% for each analysis using "Percolator". From the Sequest search output, peptide filters that included peptide confidence, peptide rank, score *versus* charge state, and search engine rank were set at the default values for proteome discoverer. In global proteome analysis, proteins were quantified label free using the peak intensity for unique and razor peptides of each protein and excluded peptides that involved methionine oxidation or phosphorylation. Phosphorylated peptides were analyzed based on peptide-spectrum matches.

7. Statistical analysis

Raw data for the average number of technical replications for each sample were log2-transformed and normalized by width adjustment. Sample groups were compared by ANOVA tests with Benjamini-Hochberg correction using Perseus software (version 1.6.10.50) [6].

Results were visualized using RStudio (version 1.3.1093), a component of R software (version 3.6.0). Other software packages included factoextra for principal component analysis (PCA), PerformanceAnalytics for correlation plotting, ggplot2 for drawing boxplots, 2D plots of points, and pheatmap for drawing heatmaps.

8. Pathway analysis

Signaling pathways based on proteins were analyzed by hallmarks in the Molecular Signatures Database (MSigDB) [7] following rapid integration of term annotation and network resources [8], WikiPathways [9] on the Enrichr [10]. PathVisio 3 [11] was used to draw the androgen receptor (AR) network in PCa.

RESULTS

1. Comparative proteome analysis workflow

Nine tissue samples were collected from three patients with prostate diseases. Three samples were collected from each patient, differing in TUR-P energy parameters, the location of prostate tissue and the presence of heat damage due to biopsy direction (Fig. 1). The characteristics of the three patients are summarized in Table 1. Three samples at approximately the same location within the prostate were obtained from PCa Pt1, labeled prostate tissue #1, differing by TUR-P current power parameters, *i.e.*, cutting and coagulation currents of 40 W and 0 W, 60 W and 0 W, and 60 W

and 40 W, respectively. Three samples at different sites within the prostate were obtained from BPH Pt2 at TUR-P cutting and coagulation currents of 60 W and 40 W, respectively. The three tissue samples obtained from PCa Pt3 included samples on the inner and outer surfaces of the prostate, with the inner sample having no thermal damage due to the surgical instrument and the outer sample having thermal damage.
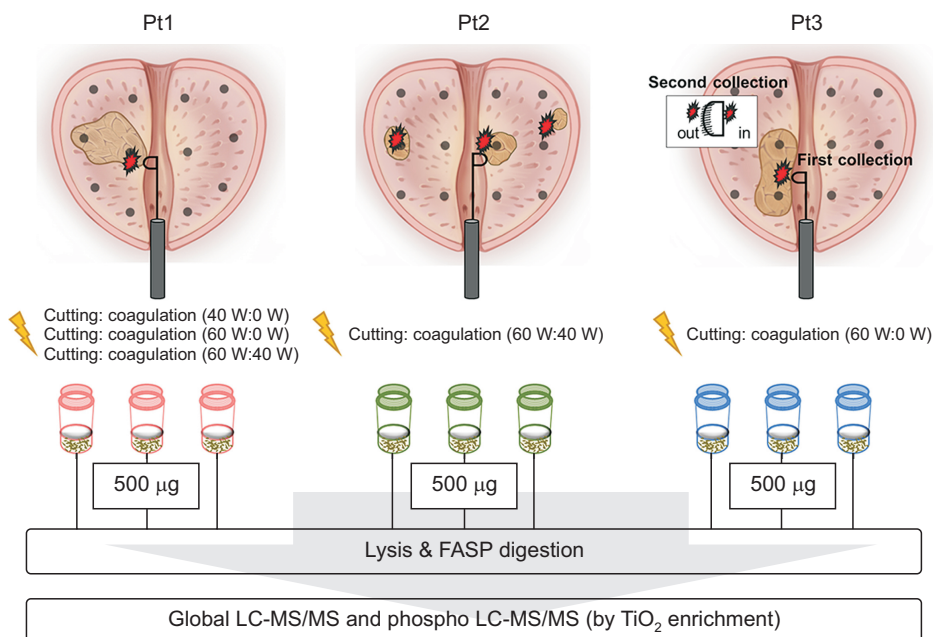
2. Global proteomic analyses

The global proteomes of these nine tissue samples were analyzed by triplicate LC-MS/MS. A total of 6,019 proteins were identified, and 3,410 proteins were completely quantified in 18 of the LC-MS/MS runs. The PCA plot shows that the differences among individual proteomes were greater than the differences associated with the biopsy method (Fig. 2A). Pearson correlation analysis showed a high correlation among

Table 1. Baseline characteristics of the patients

Characteristic	Patient #1	Patient #2	Patient #3
Diagnosis	PCa	BPH	PCa
Age (y)	60	75	64
PSA (ng/mL)	218	1.49	1,035
Gleason score	4+5		5+4
Clinical TNM stage	T3bN0M1		T4N1M1

PSA: prostate-specific antigen, PCa: prostate cancer, BPH: benign prostatic hyperplasia.

Cutting: coagulation (40 W:0 W)
Cutting: coagulation (60 W:0 W)
Cutting: coagulation (60 W:40 W)

Cutting: coagulation (60 W:40 W)

Cutting: coagulation (60 W:0 W)

500 μg

500 μg

500 μg

Lysis & FASP digestion

Global LC-MS/MS and phospho LC-MS/MS (by TiO$_2$ enrichment)

Fig. 1. Experimental workflow. Tissue samples from transurethral resection of the prostate (TUR-P) needle core biopsy were sonicated, stored at -80℃, and subsequently lysed for filter-aided sample preparation (FASP) digestion. Some of the peptides were directly subjected to global proteome analysis and the rest for enrichment using TiO$_2$ for phosphoproteome analysis. Each digested peptide sample was analyzed by LC-MS/MS. Pt: patient.
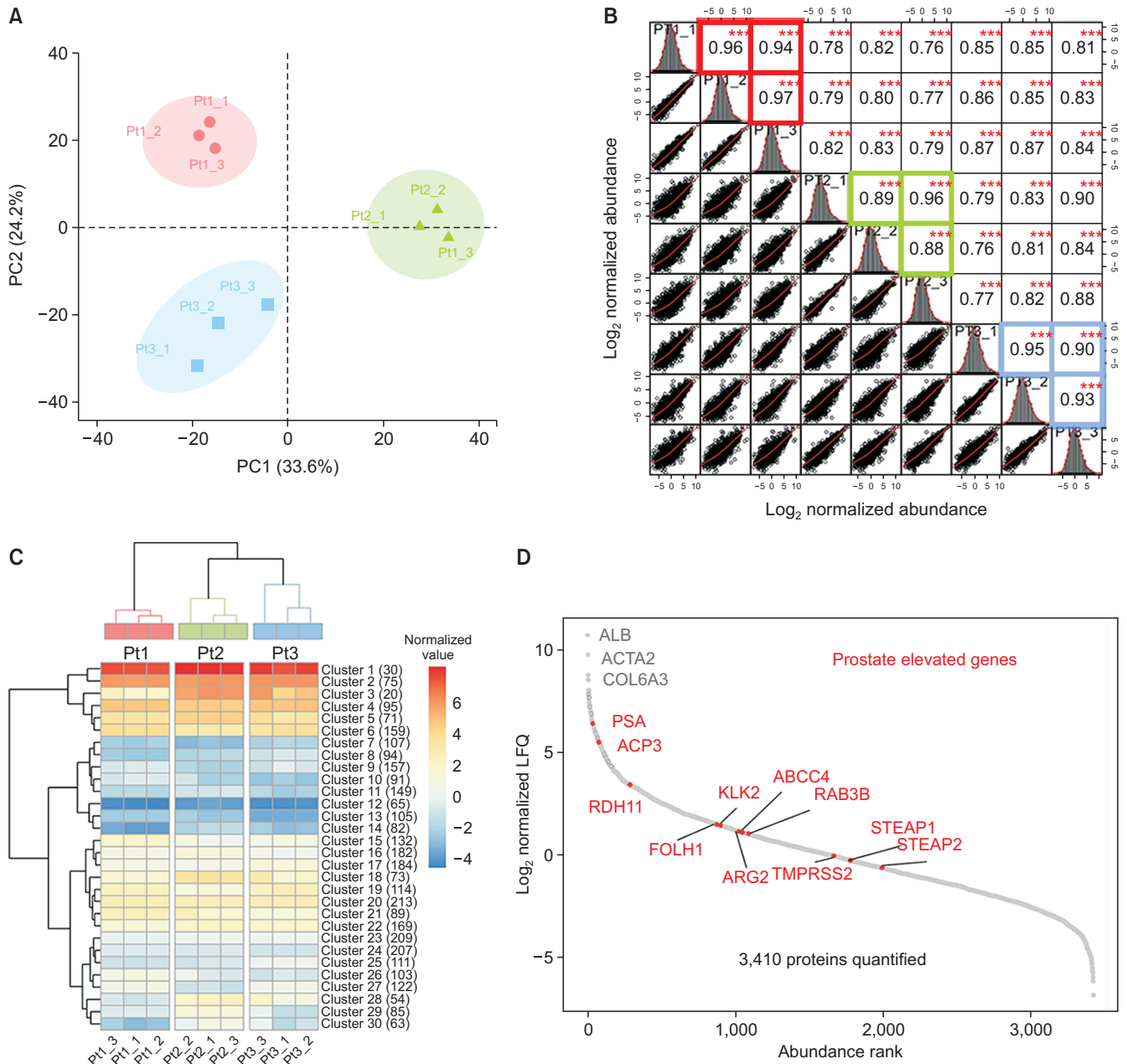
Fig. 2. (A) Principal component analysis of the global proteome of the nine tissue samples obtained from the three study patients. (B) Correlation plot of the nine samples. (C) Hierarchical clustering of the nine samples. (D) Distribution of protein abundances based on label-free quantification. Prostate-elevated proteins are highlighted in red. Pt: patient, LFQ: lable-free quantification. ***$p<0.05$.

them ($\rho>0.76$), with the protein abundances of samples within individuals having higher correlation values ($\rho_{within-PT1}>0.94$, $\rho_{within-PT2}>0.88$, $\rho_{within-PT3}>0.90$) than that of samples between individuals (Fig. 2B). The heatmap also found that the within-subject variation of protein abundance is less than the between-subject variation (Fig. 2C). Comparisons with the Human Protein Atlas (https://www.proteinatlas.org/) showed that, of the 3,410 completely quantified proteins, 11 were elevated in prostate tissue samples (Fig. 2D).

3. Individually differentiated global proteomic analysis

Differentiating global proteins in each patient that were detected by ANOVA test with Benjamini–Hochberg correction (adjusted p-value<0.05) and presented as a heat map were divided into two clusters, based on whether they increased or decreased (Fig. 3A).
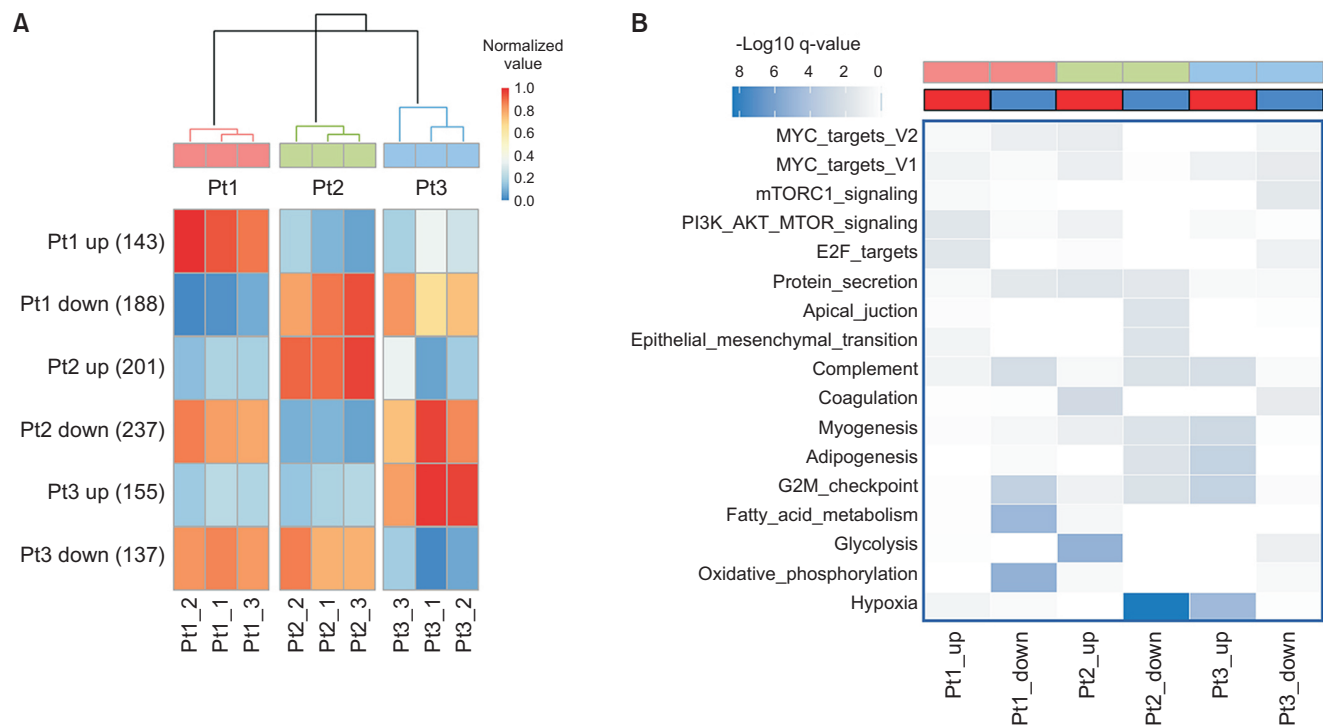
Fig. 3. (A) Hierarchical clustering of prostate tissue proteins in the nine tissue samples. (B) Functional enrichment analysis of proteins specifically upregulated in the three patients using the Molecular Signatures Database hallmark gene set. PT: patient.

These six protein clusters were mapped to the MSigDB hallmarks collection (Fig. 3B), a functional annotation database. Proteins associated with hypoxia, a characteristic of cancer cells, were found to be highly expressed in the two PCa patients (Pt1 and Pt3), especially Pt3, but to a lower extent in benign prostate tissue of the patient with BPH (Pt2). Conversely, the levels of expression of proteins involved in oxidative phosphorylation were low in Pt1 and Pt3, but high in Pt2. This finding was consistent with the Warburg effect, in which cancer cells grow through glycolysis, and oxidative phosphorylation and fat metabolism are turned off by converting pyruvate to lactate [12]. The levels of proteins associated with fatty acid metabolism were decreased in Pt2 and altered in Pt3 [13]. However, proteins related to glycolysis are highly expressed in Pt2, but to a lower extent in Pt3. The higher expression of proteins associated with glycolysis in BPH than in PCa is related to the characteristics of prostate tissue that produces sperm. Citrate is formed by oxaloacetate bound to acetyl CoA, which is converted by pyruvate produced by glycolysis and plays an import role in sperm motility within the prostate [14]. The level of citrate in BPH tissue, 8,000 to 15,000 nmol/g, is similar to that of normal tissue, but is 16 to 30 times higher than the level in malignant prostate tumors, 500 nmol/g [15]. Proteins involved in the PI3K-AKT-mTOR, MYC, and E2F signaling pathways were found to be elevated in Pt1, proteins involved in mTORC1 were elevated in Pt2, and proteins in the MYC and mTORC1 pathways were highly increased in Pt3. Proteins involved in the cell cycle were increased in Pt1 and proteins associated with coagulation [16], complement [17], adipogenesis, apical junction, and myogenesis were increased in Pt2.

4. Phosphoproteomic analyses

Proteomic analyses identified 4,280 phosphorylated peptides, with ~87% being singly phosphorylated, ~12% being doubly phosphorylated, and ~1% being triply phosphorylated. About 85% of the phosphorylated residues was serine, although ~4% were threonine and ~1% were tyrosine residues (Fig. 4A). Similar to global proteome results, PCA and Pearson correlation plots showed that inter-individual differences were greater than intra-individual differences (Fig. 4B). Pearson correlation analyses showed that protein abundance of tissue samples within each individual patient was more highly correlated than protein abundance of samples obtained from different patients ($\rho_{\text{within-PT1}} > 0.83$, $\rho_{\text{within-PT2}} > 0.90$, $\rho_{\text{within-PT3}} > 0.75$; Fig. 4C). The 30-means

phosphorylated peptide clusters represented variations between individuals rather than variations based on differently obtained samples within each patient (Fig. 4D). The relative within-subject difference was in the order Pt3>Pt1>Pt2. However, the top four phosphorylated proteins clusters were involved in many oncogenic pathways, including the AR, Notch, TGF-beta, and VEGFA-VEGFR2 signaling pathways (Fig. 4E) [10].

5. Androgen receptor network in prostate cancer

The growth of recurrent PCa cells mainly depends on the AR-signaling pathway, which is a target for androgen deprivation therapy [3] and changes during PCa progression [18]. This study identified and quantified 47 global proteins and 30 phosphorylation sites of

14 proteins found to be involved in the AR network in PCa, considered the WikiPathway WP2263 [9]. The quantitative profiling values of phosphorylated and global proteins in these nine samples were mapped to the AR pathway (Fig. 5). The expression of the nuclear receptor AR differed among the three Pt2 samples, which differed by site within the prostate. The levels of global and phosphorylated proteins stimulated by AR, including FKBP5, KLK3 (also called PSA), KLK2, NDRG1, and ABCC4, did not differ markedly among the three samples taken from individual patients, although one phosphorylated peptide of ABCC4 was lower in one Pt1 sample than in the other two. Overall, protein abundances of samples within individuals were more highly correlated than protein abundances of samples between individuals ($\rho_{\text{within-PTl}}>0.858$,
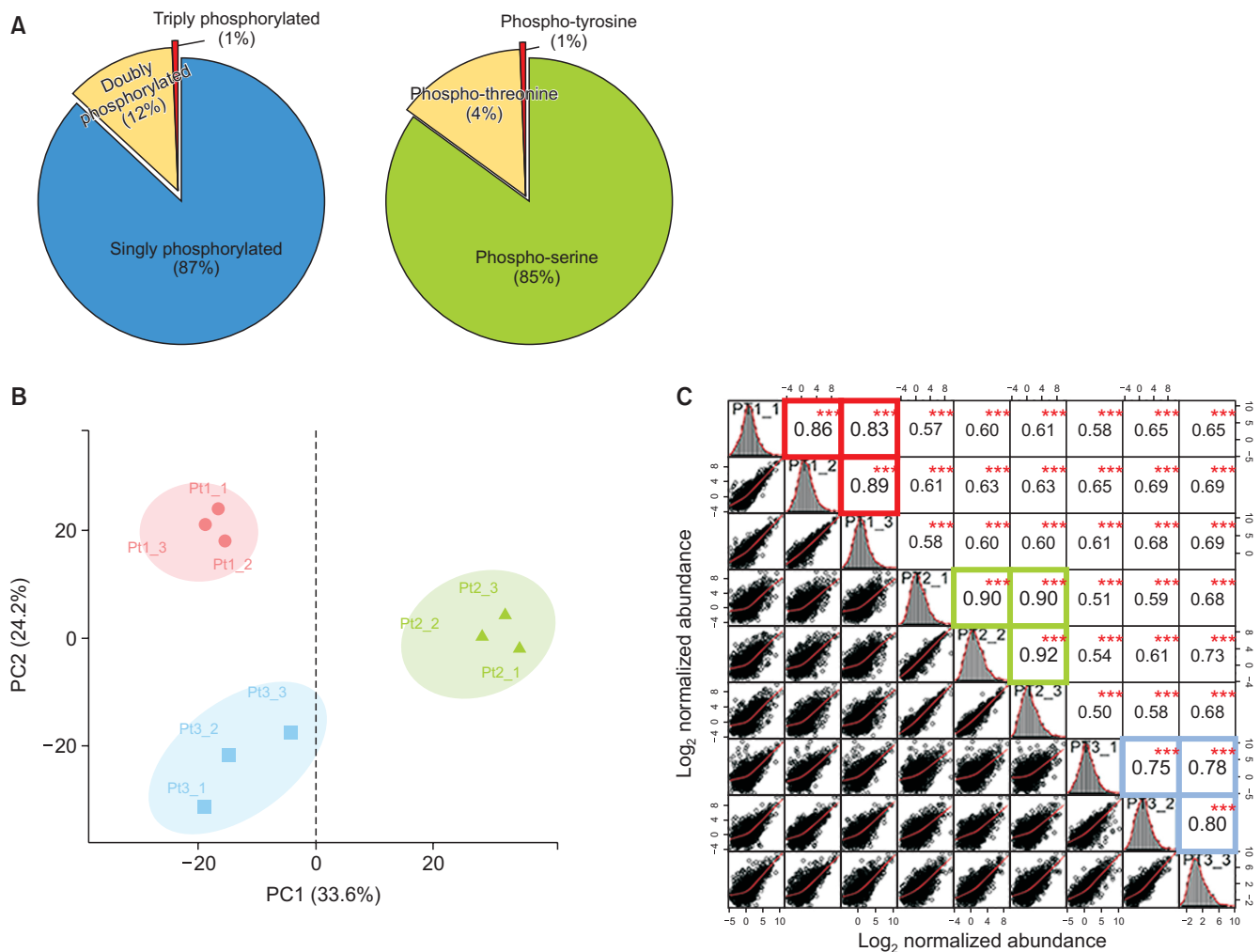
Fig. 4. Unbiased and in-depth mass spectrometry results of the phosphoproteome. (A) Pie charts showing the probability of phosphosites measured, the number of phosphosites per peptide, and the distribution of amino acid residues of phosphopeptides. (B) Principal component analysis (PCA) plot of the nine samples obtained from three patients. (C) Correlation plot of the nine samples. (D) Hierarchical clustering in nine samples. (E) Association between signal pathways and proteins involved in the top four clusters in WikiPathways of Enrichr. Pt: patient. ***p<0.05.
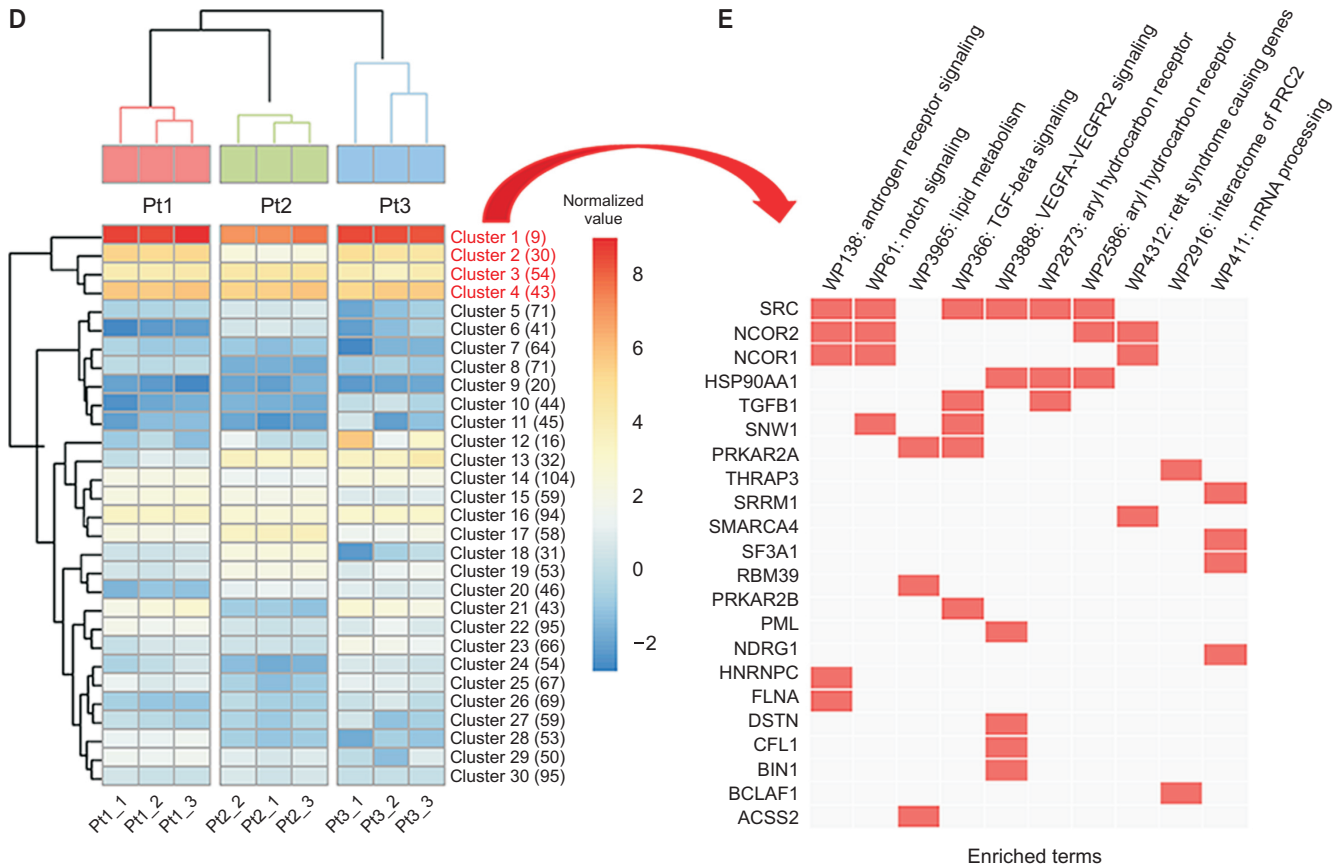
D

E

Fig. 4. Continued.

$\rho_{within-PT2} > 0.859$, $\rho_{within-PT3} > 0.849$).

DISCUSSION

Many researchers investigating with PCa have a common obstacle to proceed the study. That is the sample. Prostate is a relatively small organ, therefore, the volume of PCa is very small if localized PCa. Even though advanced PCa, CRPC, is relatively bigger, but the PCa usually represents multifocality. In addition, there was no report about sample preparation of prostate tissues (standard of procedure). We usually get the samples from prostate with prostate biopsy or surgery including prostatectomy or TUR-P. TUR-P is a very useful method to get large amount of tissues but this surgery is performed with electrical currents, which means this procedure may cause protein denaturation. In this study, we investigated protein quality with samples from TUR-P with different current conditions.

The present study assessed the effects of surgical condition on protein abundance in prostate tissue samples obtained from individual patients. Quantitative analysis found that the tissue-specific propensity of the prostate itself remains intact, regardless of surgical parameters, with differences between individuals being greater than the differences within individuals. Quantitative proteome analysis found that the three samples obtained from each patient under different conditions retain the general characteristics of prostate tissue, with the samples from the two PCa patients showing similarly high expression of cancer phosphorylation signaling pathways. Surgical conditions, however, were found to alter the expression of some proteins with relatively low phosphorylation levels. Two of the 30 clusters of phosphorylated proteins (#11, #12) differed among the three tissue samples obtained from each individual patient. The phosphorylation of proteins in these clusters, including ACSS2-S30, PRKAB1-S108, PRKAB2-S108, and PRKAR2B-S114, was significantly associated with the lipid metabolism pathway (WP3965). Phosphorylation of some proteins involved in AMPK-mediated regulation of lipid metabolism was altered by surgical techniques. Thermal changes due to TUR-P, however, did not affect the global and phos-
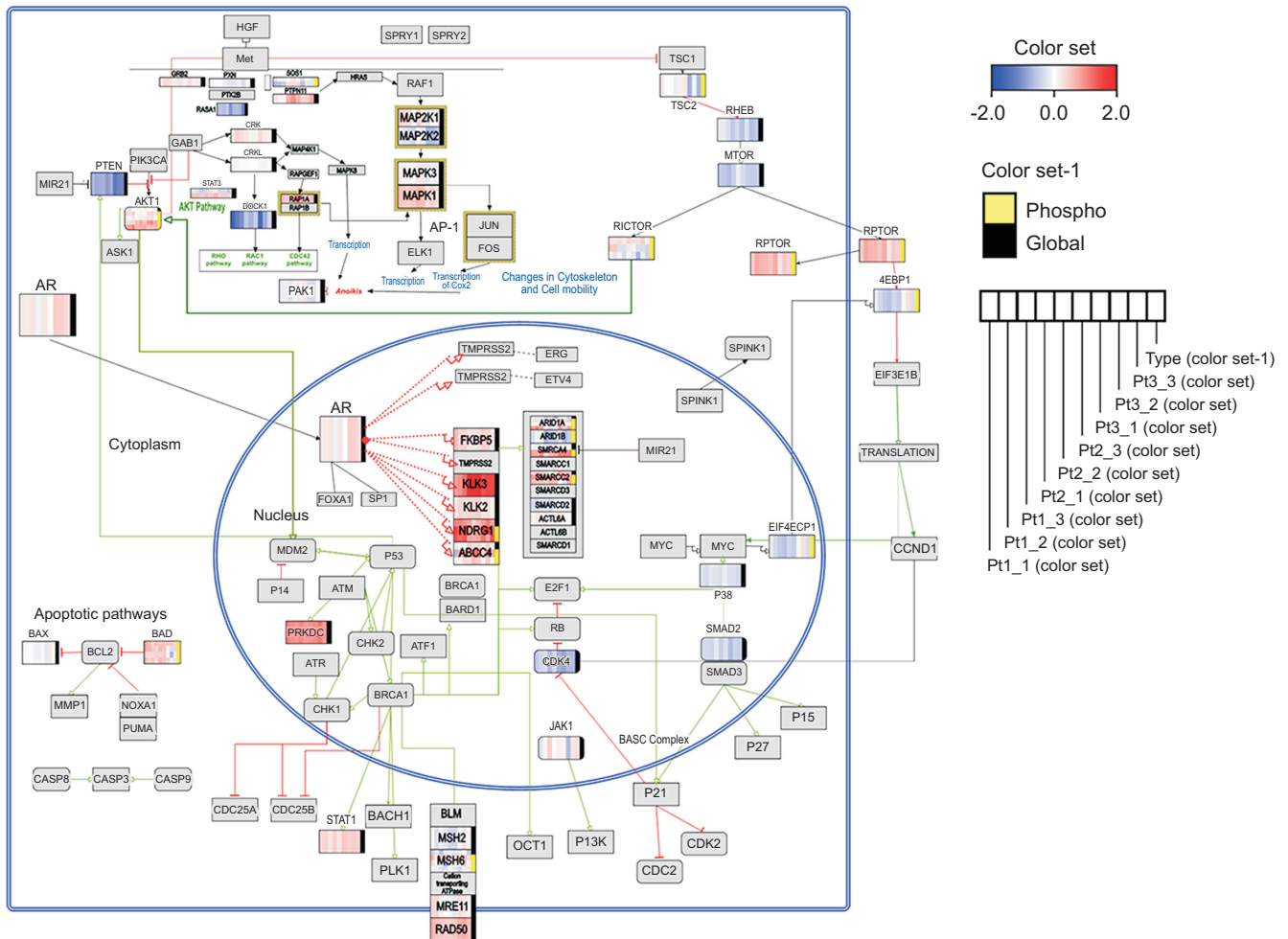
Fig. 5. Molecular interaction map designed in PathVisio for the nine tissue samples obtained from three patients for the androgen receptor network in prostate cancer (WikiPathway: WP2263). Expression is reported as the $\log_2$ relative abundance of each relevant gene in the nine samples, with red indicating protein upregulation, green indicating protein downregulation, and gray indicating the absence of data. In color set-1, yellow indicates phosphorylated peptides and black indicates global peptides. Pt: patient.

phorylation profiles of heat shock proteins, suggesting that acute exposure to the TUR-P device did not last long enough to affect the homeostasis responses of heat shock proteins.

Although three prostate tissue samples were collected from each patient, analyses of small numbers of tissue samples have limitations. Because samples biopsied or prostatectomied are less likely to be thermally damaged compared with TUR-P, this result will be a very fundamental data for future research including protein analysis using PCa samples, especially CRPC.

CONCLUSIONS

This study assessed whether alterations in needle biopsy parameters had a significant impact on global and

phosphorylated protein expression. Proteomic analysis showed that, although technical differences altered proteomic profiles somewhat, these differences were not as great as differences observed between individual patients. These results indicate that needle biopsy can be used for proteomic analysis without correcting for parameters associated with tissue sampling.

Conflict of Interest

The authors have nothing to disclose.

Funding

Author Contribution

Conceptualization: HKH, KK. Data curation: HSA, HKH. Formal analysis: JY, HJ, HSA. Funding acquisition: HKH, KK. Investigation: HKH, KK. Methodology: HJ, JYK, WYP. Project administration: HKH, KK. Resources: BJK, KHK. Software: HSA. Supervision: HKH, KK. Validation: HSA, CHL, SS. Visualization: HSA. Writing – original draft: HSA, SSB. Writing – review & editing: HSA, HKH, SSB.

Data Sharing Statement

The data analyzed for this study have been deposited in HARVARD Dataverse and are available at https://doi.org/10.7910/DVN/RDIPUV.

REFERENCES

1. Sung H, Ferlay J, Siegel RL, Laversanne M, Soerjomataram I, Jemal A, et al. Global cancer statistics 2020: GLOBOCAN estimates of incidence and mortality worldwide for 36 cancers in 185 countries. CA Cancer J Clin 2021;71:209-49.

2. Hoffman RM. Clinical practice. Screening for prostate cancer. N Engl J Med 2011;365:2013-9.

3. Yang W, Freeman MR, Kyprianou N. Personalization of prostate cancer therapy through phosphoproteomics. Nat Rev Urol 2018;15:483-97.

4. Latonen L, Afyounian E, Jylhä A, Nättinen J, Aapola U, Annala M, et al. Integrative proteomics in prostate cancer uncovers robustness against genomic and transcriptomic aberrations during disease progression. Nat Commun 2018;9:1176.

5. Schaeffer E, Srinivas S, Antonarakis ES, Armstrong AJ, Bekelman JE, Cheng H, et al. NCCN guidelines insights: prostate cancer, version 1.2021. J Natl Compr Canc Netw 2021;19:134-43.

6. Tyanova S, Cox J. Perseus: a bioinformatics platform for integrative analysis of proteomics data in cancer research. Methods Mol Biol 2018;1711:133-48.

7. Subramanian A, Tamayo P, Mootha VK, Mukherjee S, Ebert BL, Gillette MA, et al. Gene set enrichment analysis: a knowledge-based approach for interpreting genome-wide expression profiles. Proc Natl Acad Sci U S A 2005;102:15545-50.

8. Zimmermann MT, Kabat B, Grill DE, Kennedy RB, Poland GA. RITAN: rapid integration of term annotation and network resources. PeerJ 2019;7:e6994.

9. Martens M, Ammar A, Riutta A, Waagmeester A, Slenter DN, Hanspers K, et al. WikiPathways: connecting communities. Nucleic Acids Res 2021;49:D613-21.

10. Chen EY, Tan CM, Kou Y, Duan Q, Wang Z, Meirelles GV, et al. Enrichr: interactive and collaborative HTML5 gene list enrichment analysis tool. BMC Bioinformatics 2013;14:128.

11. Kutmon M, van Iersel MP, Bohler A, Kelder T, Nunes N, Pico AR, et al. PathVisio 3: an extendable pathway analysis toolbox. PLoS Comput Biol 2015;11:e1004085.

12. Eidelman E, Twum-Ampofo J, Ansari J, Siddiqui MM. The metabolic phenotype of prostate cancer. Front Oncol 2017;7:131.

13. Schöpf B, Weissensteiner H, Schäfer G, Fazzini F, Charoentong P, Naschberger A, et al. OXPHOS remodeling in high-grade prostate cancer involves mtDNA mutations and increased succinate oxidation. Nat Commun 2020;11:1487.

14. Peitzsch C, Gorodetska I, Klusa D, Shi Q, Alves TC, Pantel K, et al. Metabolic regulation of prostate cancer heterogeneity and plasticity. Semin Cancer Biol 2020. doi: 10.1016/j.semcancer.2020.12.002 [Epub].

15. Costello LC, Franklin RB. The intermediary metabolism of the prostate: a key to understanding the pathogenesis and progression of prostate malignancy. Oncology 2000;59:269-82.

16. Desai M, John B, Evans G, Eddy B. Prostate cancer: beware of disseminated intravascular coagulation. BMJ Case Rep 2015;2015:bcr2014206814.

17. Pio R, Corrales L, Lambris JD. The role of complement in tumor growth. Adv Exp Med Biol 2014;772:229-62.

18. Culig Z, Santer FR. Androgen receptor signaling in prostate cancer. Cancer Metastasis Rev 2014;33:413-27.